• Clinical Research •

Choroidal response to optical defocus as a potential surrogate marker for myopia control effect

Muteb K. Alanazi[1], Mohammed Alshehri[1], Mohammed Althomali[1], Mohammed Alhazmi[1], Mansour Alghamdi[1], Nawaf M. Almutairi[2], Basal Altoaimi[1], Ahmed Alharbi[1], Ali Almustanyir[1], Maria Liu[3]

[1]Optometry Department, College of Applied Medical Sciences, King Saud University, Riyadh 11451, Saudi Arabia
[2]Department of Optometry, College of Applied Medical Sciences, Qassim University, Buraydah 51452, Saudi Arabia
[3]UC Berkeley School of Optometry, Berkeley 94720, California, United States
Correspondence to: Muteb K. Alanazi. Optometry Department, College of Applied Medical Sciences, Office 2096, Building 24, King Saud University, Riyadh 11451, Saudi Arabia. mkalanazi@ksu.edu.sa
Received: 2024-09-20 Accepted: 2025-04-16

Abstract

● **AIM:** To investigate short-term changes in choroidal thickness in response to peripheral myopic defocus induced by two designs of multifocal corneal gas permeable contact lenses (MFGPCL) in young adults.

● **METHODS:** Seventeen participants, with a mean age of 24.5±4y, underwent choroidal thickness and vascularity index measurements using enhanced depth imaging optical coherence tomography (EDI OCT) at baseline, one day, and one week following MFGPCL wear. Two center-distance MFGPCL designs with similar center zone diameters of 3.0 mm but different peripheral add powers (low add: +1.5 D and high add: +3.0 D) were tested. Each participant was randomly assigned to wear one of the two MFGPCL designs. Measurements of total, luminal, and stromal choroid thickness were obtained in five eccentric regions (6 mm towards the periphery) in all quadrants.

● **RESULTS:** Significant thickening in total choroidal thickness were observed after one week of wearing both high add (+10±6 μm) and low add (+7±5 μm) MFGPCLs, with no statistically significant difference between the two groups (P=0.42). Choroidal thickening was consistent across eccentric regions and quadrants, with no significant differences based on eccentricity or quadrant (all P>0.05). Both lens designs induced choroidal thickening, with no significant difference between them in total choroidal thickness (P=0.18 for quadrants, P=0.51 for eccentric regions).

● **CONCLUSION:** Peripheral myopic defocus induced by MFGPCLs lead to significant choroidal thickening, including total, luminal, and stromal components. This study highlights the need for future research to explore the dose-response relationship between peripheral myopic defocus and choroidal thickening, utilizing choroidal response as a potential biomarker.

● **KEYWORDS:** choroid; choroidal vascularity index; gas-permeable contact lens; myopia
DOI:10.18240/ijo.2025.08.15

Citation: Alanazi M, Alshehri M, Althomali M, Alhazmi M, Alghamdi M, Almutairi N, Altoaimi B, Alharbi A, Almustanyir A, Liu M. Choroidal response to optical defocus as a potential surrogate marker for myopia control effect. *Int J Ophthalmol* 2025;18(8):1529-1536

INTRODUCTION

Myopia poses a significant threat to vision worldwide due to the dramatic increase in myopia prevalence and its links to vision-threatening conditions such as myopic macular degeneration[1], posterior staphyloma, glaucoma[2] retinal detachment[3], and cataract[4]. Clinically significant myopia control strategies have been developed to reduce myopia progression rate among children, including pharmaceutical agents (*i.e.*, atropine)[5] and optical treatments, such as multifocal contact lenses[6] and orthokeratology[7].

Both central and peripheral retina contribute to refractive error development and ocular growth. From experiments that were conducted on infant monkeys, excessive axial elongation and myopia progression occur in primates with form deprivation or hyperopic blur applied outside the macula. Even if the macula is ablated[8], axial elongation slows, and the amount of imposed myopia decreases after the stimulus to accelerate eye growth is removed. Compared to emmetropic or hyperopic eyes, myopes show more relative peripheral hyperopia[9]. This relative peripheral hyperopia precedes the development of myopia, indicating that relative hyperopic defocus may be a factor in the development of myopia[10]. Furthermore, in

a prior multifocal contact lens myopia control trial, reduced relative peripheral refractive error was linked to a slower rate of myopic progression[11].

Changes in axial length (AL) and refractive error are typically the primary outcomes in clinical trials that explore the efficacy of myopia control treatments. However, both variables take a long time to detect a clinically meaningful difference, making the clinical studies time-consuming, expensive, and subject to high dropout rates.

From recent findings, the long-term changes in AL and refraction are found to be correlated with short-term ocular changes that take place at levels of the retina and choroid[12-14]. More recent studies on humans and animals have shown that the choroid plays a crucial part in the local development process of the eye. It is conceivable that the choroid participates in a signalling cascade that starts in the retina and eventually results in long-term modifications to scleral and ocular growth[15].

Studies that included animal models have shown myopic defocus, which eventually leads to myopia retardation and slowed elongation rate, induced choroidal thickening minutes after exposure to the imposed myopic defocus[16]. On the other hand, imposed hyperopic defocus, which leads to accelerated ocular growth and myopia progression, induces choroidal thinning that far preceded the changes in refraction and AL[17-20]. The observed bidirectional choroidal response to optical defocus has been demonstrated in humans[21]. Several studies reported a significant short-term choroidal response associated with certain myopia control interventions such as atropine[22] and orthokeratology[23-25].

The short-term changes in response to defocus are not limited to changes in choroidal thickness (CT). Several studies explored bidirectional short-term changes happening in choroidal blood flow in animals. Experimentally induced myopia (*i.e.*, form deprivation and lens-induced) reported a significant decrease in CT and choroidal blood perfusion, which was more predominant in form deprivation models[26].

In this study, we explored the changes in CT and vascular index as a short-term response to peripheral myopic defocus using high and low add multifocal corneal gas permeable contact lens (MFGPCL) designs (*i.e.*, +3.0 and +1.5 D add power).

PARTICIPANTS AND METHODS

Ethical Approval All participant provided their written consent form before the study sessions began. The study was approved by the institutional review board, and its procedures adhered to the tenets of the Declaration of Helsinki. Only participants with best-corrected distance visual acuity 0.0 logMAR with astigmatism less than 2.0 D were eligible to participate. Anisometropia was an exclusion criterion, ensuring that participants had similar refractive errors in both eyes. All participants had never undergone ocular surgery, and neither did they take any systemic or topical medications that are known to be contraindicated with contact lens wear.

Participants In this study, a total of 17 healthy young adults [age mean±standard deviation (SD): 24.5±4] were recruited. Only participants with best-corrected distance visual acuity 0.0 logMAR with astigmatism less than 2.0 D were eligible to participate. Anisometropia was an exclusion criterion, ensuring that participants had similar refractive errors in both eyes. All participants had never undergone ocular surgery, and neither did they take any systemic or topical medications that are known to be contraindicated with contact lens wear.

Data Collection Procedure After confirming the participants' eligibility, non-cycloplegic auto-refraction, AL data, the corneal topographical data were obtained using OPD scan III, IOLMaster 500 (Zeiss, Germany), and Medmont E300 corneal topographer (Medmont Pty, Ltd., Melbourne, Australia), respectively. Subjective refraction was performed to determine the participant's best refractive correction. All participants were randomly assigned to wear and be tested with one of the two experimental multifocal lenses (high add or low add) binocularly every day for seven days. The choroid measurements were taken three times (*i.e.*, at baseline, after 4 to 5h following lens wear on the first day, and after completing seven days of lens wear). Participants were instructed to wear the contact lenses daily during the waking hours.

Measurements

Corneal gas-permeable contact lens designs The optical designs of the two tested multifocal gas-permeable contact lenses had central and peripheral zones. The central zone of both designs had a fixed diameter of 3 mm which contained the participant's distant correction that was obtained through subjective refraction. Two add powers were incorporated in the peripheral zone, low (1.5 D) and high add power (3.0 D; Figure 1). The lens parameters, such as the central diameter, peripheral zone size, and power, were confirmed using the Rotlex Contest 2 (Rotlex Instruments, Israel). The overall lens diameter was customized to be 0.80 mm smaller than the participant's horizontal visible iris diameter (HVID). Both lens designs had a refractive index of 1.415 and were made of Boston XO (Hexafocon A) material with a permeability (Dk) of 100 (ISO/FATT cgs unit).

Choroidal thickness Participants' right eyes were examined using a spectral domain optical coherence tomography SD-OCT (Optovue Inc., Freemont, CA, USA) using the enhanced depth imaging (EDI) mode. Choroidal imaging was obtained by taking three single 12-mm high-resolution per horizontal meridian and three per vertical meridian. Each scan has a resolution of 496 pixels per A-scan and 1024 A-scans per

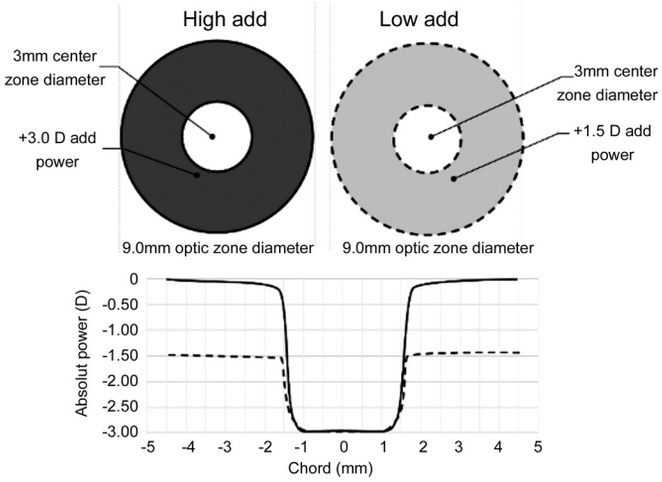

Figure 1 Schematic diagrams showing the geometric optical zones of MFGPCL designs used in the study MFGPCL: Multifocal corneal gas permeable contact lenses.

B-scan. Each scan was centred on the foveal pit. Each single line scan had a minimum of 60 averaged B-scans. To ensure the scan quality and positioning, real-time eye-tracking instrument feature was used. Scans with the best visualization of choroidal boundaries were chosen for analysis.

The CT was quantified automatically using software developed by Alonso-Caneiro *et al*[27] and Read *et al*[28]. Studies have shown that differences in CT exist at each quadrant and eccentricity[29], where the superior choroid exhibited the highest thickness and the nasal choroid showed the thinnest. Due to the observed significant variation in CT based on location, the data was recorded and analysed for each location separately. In each quadrant, the CT measurements were divided into five anatomical areas (fovea, parafovea, perifovea, near-periphery and periphery; Figures 2A and 2C). The software contained image contrast enhancement that improved the visualization of the choroidoscleral junction[30].

To minimize the impact from major known confounders to CT, such as physical activity[31], near work[32], and light[33], subjects were asked to spend 15min prior to the measurements in a room with a low ambient light level while looking at a distant target placed at 3 m. The OCT scans were obtained while subjects wore the MFGPCLs, as previous studies have demonstrated the minimal impact of contact lens wear on OCT imaging of thickness parameters[34-35]. To control for the physiologic diurnal variation in CT, measurements were collected within the same time window during the day (*i.e.*, from 10 *a.m.* to 12 *p.m.*) at baseline and follow-up visits.

Choroidal vascularity index All B-scan segmented scans were binarized using the Niblack local binarization method in MATLAB, developed by the Contact Lens and Visual Optics Laboratory at Queensland University of Technology, Australia. This algorithm was used and reported by Yazdani *et al*[36] and Alanazi[37].

Based on the OCT scans, the software generates over 1900 choroidal vascularity index (CVI) data points that were averaged over the predetermined eccentricities for each OCT scan. The luminal CT (defined as CVI×CT) and the stromal CT (defined as CT–luminal thickness) across various eccentricities were calculated using the CVI. An experienced observer chose the window size for image binarization based on preserving it to be both small enough to preserve the choroidal vascularity details and large enough to cover the luminal and stromal components, as stated by Yazdani *et al*[36] and Alanazi[37]. The average window size selected by the experienced observer was 29±5.1 pixels for horizontal scans and 31±5.1 pixels (Figure 2B and 2D). Prior to obtaining the total CT and CVI data from OCT scans, the transverse scaling of each scan was adjusted based on participants' AL data to take the effect of ocular magnification into account, as explained by Read *et al*[38].

Peripheral refraction Peripheral refraction measurements were acquired using an open-field Auto-Refractometer WAM-5500 (Grand Seiko Co, Ltd, Hiroshima, Japan) extending up to 25 degrees in the nasal and temporal fields in 5-degree increments. Head turn method was used to minimized the contact lens decentration and better maintained the contact lens in the primary gaze position. At least three readings were collected at each eccentric location while the subject was maintaining the primary gaze. Each measurement was captured 1 to 2s after a blink to allow the lens re-centration and settlement. A Maltese cross placed at a 2.5-meter distance was used to as a fixation target, featuring horizontal grating lines equivalent to 0.1 logMAR with 100% contrast.

In order to achieve the pupil dilation without significantly affecting accommodation, prior to collecting the peripheral refraction data, the examiner instilled two drops of 2.5% phenylephrine in each eye with 5min waiting time between the two drops. The subject's alignment was verified through maintaining proper forehead and chin positions. The lens centration was assessed between each measurement. The values of sphere, cylinder, and axis obtained with the autorefractometer were used to calculate spherical equivalent (SE), J0, J45 and relative peripheral refraction (RPR) values as follows

$$SE=Sph+Cy1/2$$
$$J0=–Cyl.\cos(2\alpha)/2$$
$$J45=–Cyl.\sin(2\alpha)/2$$
$$RPR=\text{eccentric SE}–\text{central SE}$$

Statistical Analysis The analysis of variance score changes was performed using SPSS version 29, including within-subject factors such as choroidal eccentricity (5 levels), quadrant (4 levels), and a between-subject factor of contact lens design (2 levels). *P* values were considered statistically significant if they were less than 0.05, and a Bonferroni

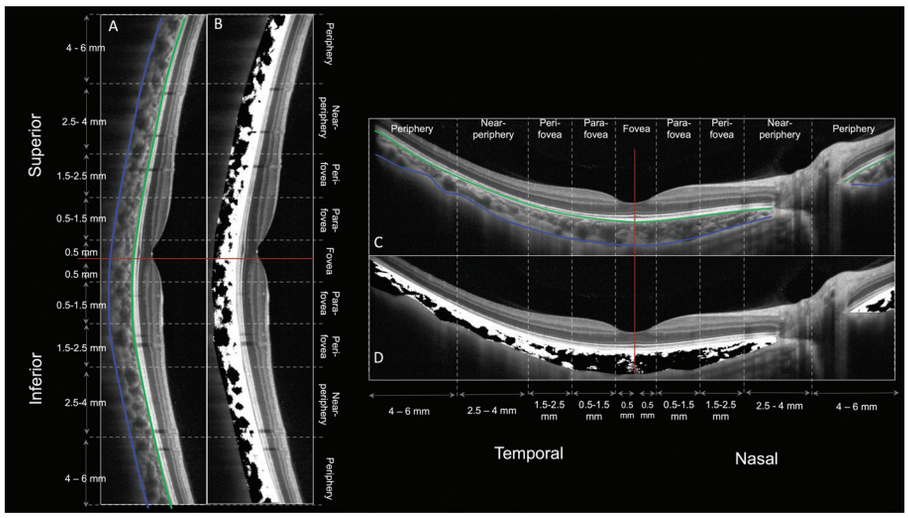

Figure 2 Vertical (A) and horizontal (C) single-line images obtained with optical coherence tomography (OCT) instrument, the foveal pit as manually marked in the custom-written software (straight red line), the anterior (green line in A and C) and posterior (blue line in A and C) are the boundaries of the choroid. In the binarized images (B and D), the dark pixels correspond to the vascular (luminal) area of the choroid, and the white pixels correspond to the stromal area.

Table 1 Participants' demographic information and baseline ocular characteristics

Parameters	High add lens	Low add lens
Sample size	8	9
Gender (female)	6	6
Age (y)	23±4.1	24±3.4
Best corrected distance visual acuity (logMAR)	-0.02±0.04	-0.02±0.02
Average corneal curvature (D)	43.8±1.3	43.6±1.1
Spherical equivalent refractive error (D)	-3.2±2.6	-3.3±2.8
Photopic pupil size (mm)	3.89±0.3	3.82±0.3
Baseline axial length (mm)	24.6±0.77	24.8 ±0.87
Baseline overall CT (μm)	257±62	252±60
Baseline superior CT (μm)	281±51	284±45
Baseline temporal CT (μm)	253±52	256±54
Baseline inferior CT (μm)	231±55	233±41
Baseline nasal CT (μm)	188±77	185±73
Baseline overall choroidal vascularity index (%)	59±6	59±5

CT: Choroidal thickness.

correction was applied for multiple comparisons when necessary.

RESULTS

Participants Demographic In this study, a total of 17 healthy young adults [age mean±standard deviation (SD): 24.5±4] were recruited. All demographic information and baseline ocular measures were summarized in Table 1.

Twenty participants were recruited, and a total of 17 young adults (12 females and 5 males) were included in this study who had completed all required visits. Eight were randomly fitted with the high add lens design (6 females), and nine participants (6 females) were randomly assigned to wear the low add lens design. There was no significant difference between the two groups in demographics and biometric ocular measures (Table 1).

The choroidal data were collected from right eyes. The overall total CT significantly thickened from baseline following 4h and one week of MFGPCL. The overall increase with high add lens was +10±6 and +7±5 μm with low add lens design with a non-significant difference (P=0.42). A significant difference in total CT on day 1 and day 7 between the two lenses was seen over one week of wearing time. High add lens design showed more thickening of +13±6 μm that was reduced to +6±4 μm on the seventh day. On the other hand, the thickening in total CT with low add lens increased from +5±4 μm on day 1 to reach +9±6 μm (Figure 3). The changes in total CT in all four quadrants were not significantly different, which indicates a similar response in all quadrants (P=0.18). Similar findings were observed with different eccentric regions, where the total choroidal thickening ranged between +7 to +10 μm (P=0.51; Figures 4 and 5).

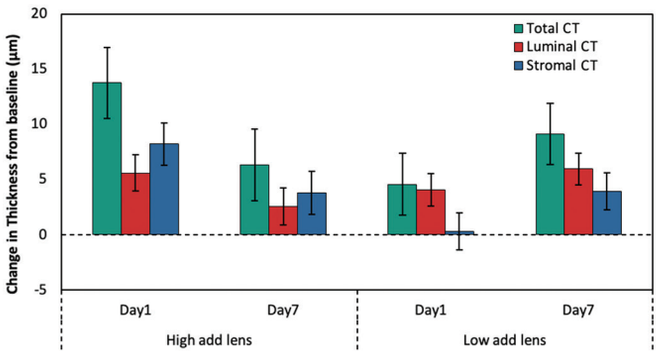

Figure 3 Mean of change in total, luminal and stromal choroidal thickness (CT) in overall measured area of choroid following 1 and 7d of lens wear Error bars represent standard error of the mean.

Both luminal and stromal choroid exhibited thickening that was not significantly different between the two lens designs (P=0.41 and 0.33, respectively; Figure 3). The thickening in both components did not differ significantly based on eccentric regions and quadrants (Figures 4 and 5).

Figure 6 showed the changes in spherical equivalence (SE) and RPR for the two gas permeable lens designs compared to baseline values (without contact lenses). Both gas permeable designs produced a statistically significant myopic shift beyond 10 degrees in the nasal (P<0.001) and temporal (P<0.001) regions compared to the no-lens condition. No significant difference was found between the high and low add gas permeable lens designs in terms of RPR within the 50° measured horizontal field. Both gas permeable lens designs also caused statistically significant changes in the J0 astigmatic component beyond 10 degrees in the nasal and temporal fields compared to baseline. However, there was no significant difference between the two designs in the J0 astigmatic component. The J45 astigmatic component remained unchanged from baseline values (P=0.73).

DISCUSSION

This study investigated the impact of two add power MFGPCL (high add of +3.0 D and low add of +1.5 D) on CT parameters, including total CT, luminal CT, and stromal CT. The study showed a significant choroidal thickening following the MFGPCL wear.

The contribution of the choroid in refractive error development and ocular elongation has been enormously reported[15]. The observed change in CT following the beginning of optical myopia treatments supports its crucial contribution to regulating ocular elongation during childhood. Several studies found a significant choroidal thickening with atropine[22] and orthokeratology[23-25].

One of the critical questions regarding optical myopia treatment strategies is whether there is a dose-response relationship. The BLINK study was the first study to investigate different doses of peripheral myopic defocus powers (+1.5 and +2.5 D)[39].

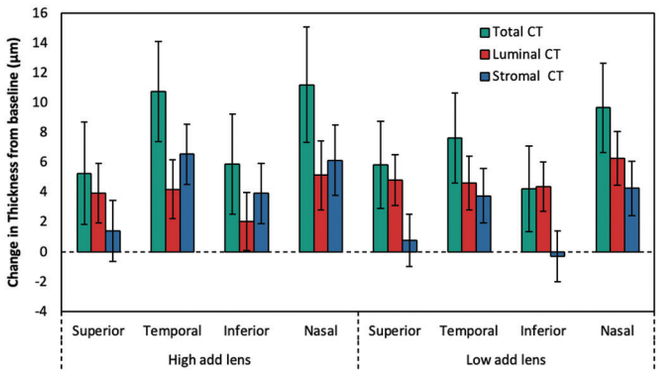

Figure 4 Mean of change in total, luminal and stromal choroidal thickness (CT) in all four measured quadrants following 1 and 7d of lens wear Error bars represent standard error of the mean.

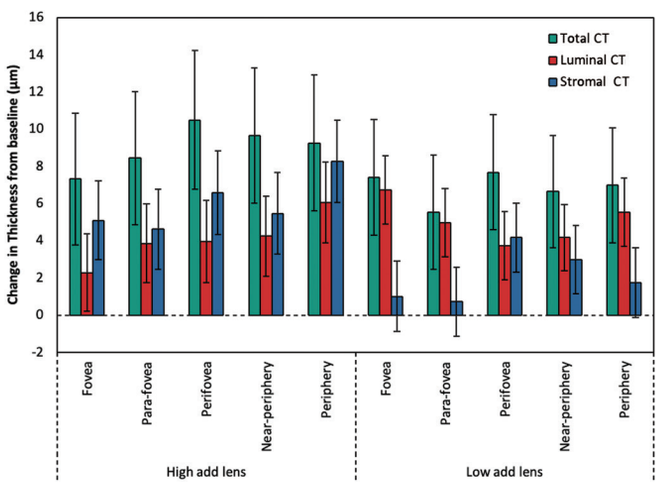

Figure 5 Mean of change in total, luminal and stromal choroidal thickness (CT) in all five measured regions of choroid following 1 and 7d of lens wear Error bars represent standard error of the mean.

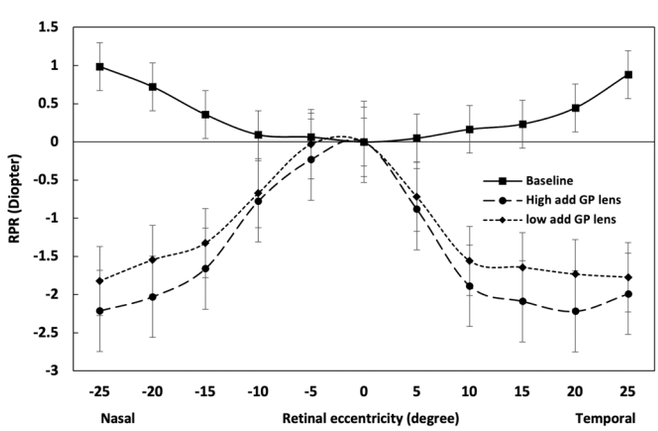

Figure 6 The change in relative peripheral refraction (RPR) across the horizontal visual field at baseline (without lenses) and for high and low add gas permeable (GP) contact lens designs The error bars indicate the standard error of the mean.

A statistically significant myopia control effect was observed with the higher add power over three years. Investigating the dose-response relationship using changes in CT as a primary outcome could provide quicker answers over a significantly shorter period of time and test different modalities of myopia management tools.

Since the choroid is primarily blood vessels, it has been hypothesized that the choroid is capable of rapid changes in its blood flow, which leads to thickness changes[26]. In studies that tested the changes in choroidal blood flow on animals with experimentally induced myopia, choroidal blood flow demonstrated bidirectional changes during form deprivation and recovery conditions. It is suggested that the hypoxia environment with reduced choroidal flow leads to a series of changes at the retinal and scleral levels contributing to myopia onset and development of ocular elongation[26,40].

Myopic eyes are known to have thinner choroid. Similarly, myopic eyes also exhibit lower blood flow, which could be explained primarily by the narrowing and increased rigidity of blood vessels. Choroidal thinning could influence the release of growth factors and increase the molecular diffusion in the scleral tissue, while the reduced blood flow affects the nourishment and oxygen supply for the scleral tissue and creating a hypoxia environment, which contributes to scleral ischaemia, possibly resulting in changes in scleral extracellular matrix remodelling, which would lead to excessive ocular elongation and ultimately accelerate myopia onset and myopia progression.

There is growing evidence that supports the rapid, short-term choroidal thickening following peripheral myopic defocus. The mechanism of peripheral myopic defocus inducing choroidal thickening remains unclear. However, the induced thickening may function as a barrier to reduce the diffusion of growth factors in the sclera or as a mechanical buffer to slow ocular elongation. Changes in CT and blood flow could be considered potential surrogate markers for the prediction of the efficacy of treatment methods for myopia.

In this study, thickening in both luminal and stromal thickness contributed to the observed total choroidal thickening. The reported choroidal blood flow changes to optically induced myopia may indicate that the majority of CT changes to optical defocus is primarily due to choroidal vasodilation or vasoconstriction. The observed changes in both luminal and stromal thickness indicate there may be fluids that being pulled into the choroid.

There were no eccentricity nor quadrant differences in the observed choroidal responses. Choroid has a topographical variation that is eccentricity- and quadrant-dependent, which can be explained by the asymmetrical distribution of choroidal vortex veins and the variation in vessels' density and diameter based on location[41-42]. It is plausible to expect a variation in the CT responses to optical defocus based on the topographical variation. With centre-distance multifocal contact lens designs, the peripheral retina and choroid are more exposed to myopic defocus than the central regions. Additionally, it has been indicated that choroid showed a localized response based on the stimulated region with hemifield spectacle lenses[43].

To our knowledge, this is the first study that investigated the change in luminal and stromal CT in addition to total CT to peripheral myopic defocus. Previous studies only reported changes in total CT as a response to optical defocus. There is no clear explanation for the inconsistency in total choroidal thickening between the two lens designs from day 1 and day 7 (*i.e.*, high add lens showed less thickening while low add lens demonstrated more thickening at day 7). Considering the limitations of the current study, future research could provide answers regarding the short-term choroidal response to peripheral myopic defocus. One limitation of this study was the small sample size (n=17) that it only included young adults, which reduced the statistical power and the generalizability of the results. Future research should include a larger sample and children with progressing myopia. Another limitation was that we did not specify a particular time of day for wearing the lenses for at least 4h daily. The CT reaction to peripheral myopic defocus could vary depending on the time of day[44]. We also did not track the time spent on visual activities that participants did, such as near-work activities while wearing the lenses. In addition, the method of obtaining CT data was based on high-resolution single-line scans of OCT images. Volumetric CT measurement provides more comprehensive and accurate data, especially when examining small changes in CT. Lastly, it may take up to 15d to achieve full adaptation with gas-permeable contact lenses[45]. Ideal future research would be to assess the choroidal response to MFGPCLs over a longer period the exceeds the required adaptation period.

In conclusion, this study showed that changes in total CT in response to peripheral myopic defocus. Short-term exposure to peripheral myopic defocus using two multifocal contact lens optical designs significantly thickened the total, luminal, and stromal choroid. The two MFGPCL designs, which differed in add power (1.5 and 3.0 D), did not show a clear dose-response relationship to peripheral myopic defocus in CT. Our results also suggest that the thickening of total CT in response to MFGPCLs is due to thickening in both the luminal and stromal layers of the choroid. The findings support that short-term changes in CT could be used as a promising surrogate marker for the long-term efficacy of myopia management tools.

ACKNOWLEDGEMENTS

Foundation: Supported by Ongoing Research Funding Program (No.ORF-2025-1160), King Saud University, Riyadh Saudi Arabia.

Conflicts of Interest: Alanazi M, None; **Alshehri M,** None; **Althomali M,** None; **Alhazmi M,** None; **Alghamdi M,** None; **Almutairi N,** None; **Altoaimi B,** None; **Alharbi A,** None; **Almustanyir A,** None; **Liu M,** None.

REFERENCES

1 Shi HK, Guo NJ, Zhao ZM, *et al*. Global prevalence of myopic macular degeneration in general population and patients with high myopia: a systematic review and meta-analysis. *Eur J Ophthalmol* 2024;34(3):631-640.

2 Ohno-Matsui K, Wu PC, Yamashiro K, *et al*. IMI pathologic myopia. *Invest Ophthalmol Vis Sci* 2021;62(5):5.

3 Cheung N, Lee SY, Wong TY. Will the myopia epidemic lead to a retinal detachment epidemic in the future? *JAMA Ophthalmol* 2021;139(1): 93-94.

4 Wei L, Zhang KK, Lu Y, Zhu X. Myopia and cataract. *Nat Cell Sci* 2023;1(1):24-31.

5 Li Y, Yip M, Ning Y, *et al*. Topical atropine for childhood myopia control: the atropine treatment long-term assessment study. *JAMA Ophthalmol* 2024;142(1):15-23.

6 Song D, Qiu W, Jiang T, *et al*. Efficacy and adverse reactions of peripheral add multifocal soft contact lenses in childhood myopia: a meta-analysis. *BMC Ophthalmol* 2024;24(1):173.

7 Lipson MJ. The role of orthokeratology in myopia management. *Eye Contact Lens* 2022;48(5):189-193.

8 Smith EL 3rd, Hung LF, Huang J. Relative peripheral hyperopic defocus alters central refractive development in infant monkeys. *Vision Res* 2009;49(19):2386-2392.

9 Mathur A, Atchison DA, Charman WN. Myopia and peripheral ocular aberrations. *J Vis* 2009;9(10):15.1-1512.

10 Mutti DO, Sinnott LT, Mitchell GL, *et al*. Relative peripheral refractive error and the risk of onset and progression of myopia in children. *Invest Ophthalmol Vis Sci* 2011;52(1):199-205.

11 Sankaridurg P, Holden B, Smith E 3rd, *et al*. Decrease in rate of myopia progression with a contact lens designed to reduce relative peripheral hyperopia: one-year results. *Invest Ophthalmol Vis Sci* 2011;52(13):9362-9367.

12 Delshad S, Collins MJ, Read SA, *et al*. Effects of brief periods of clear vision on the defocus-mediated changes in axial length and choroidal thickness of human eyes. *Ophthalmic Physiol Opt* 2021;41(4):932-940.

13 Alanazi M, Caroline P, Alshamrani A, *et al*. Impact of multifocal gas-permeable lens designs on short-term choroidal response, axial length, and retinal defocus profile. *Int J Ophthalmol* 2024;17(2):247-256.

14 Ostrin LA, Sah RP, Queener HM, *et al*. Short-term myopic defocus and choroidal thickness in children and adults. *Invest Ophthalmol Vis Sci* 2024;65(4):22.

15 Nickla DL, Wallman J. The multifunctional choroid. *Prog Retin Eye Res* 2010;29(2):144-168.

16 Zhu X, Kang P, Troilo D, *et al*. Temporal properties of positive and negative defocus on emmetropization. *Sci Rep* 2022;12(1):3582.

17 Irving EL, Callender MG, Sivak JG. Inducing myopia, hyperopia, and astigmatism in chicks. *Optom Vis Sci* 1991;68(5):364-368.

18 Irving EL, Sivak JG, Callender MG. Refractive plasticity of the developing chick eye. *Ophthalmic Physiol Opt* 1992;12(4):448-456.

19 Shen W, Sivak JG. Eyes of a lower vertebrate are susceptible to the visual environment. *Invest Ophthalmol Vis Sci* 2007;48(10):4829-4837.

20 Howlett MH, McFadden SA. Spectacle lens compensation in the pigmented guinea pig. *Vision Res* 2009;49(2):219-227.

21 Aldakhil S. The effect of optical defocus on the choroidal thickness: a review. *Open Ophthalmol J* 2021;15(1):283-287.

22 Yang Y, Wei L, Wang B, *et al*. Effects of atropine on choroidal thickness in myopic children: a meta-analysis. *Front Pharmacol* 2024;15:1440180.

23 Xiao J, Pan X, Hou C, *et al*. Changes in subfoveal choroidal thickness after orthokeratology in myopic children: a systematic review and meta-analysis. *Curr Eye Res* 2024;49(7):683-690.

24 Lee JH, Hong IH, Lee TY, *et al*. Choroidal thickness changes after orthokeratology lens wearing in young adults with myopia. *Ophthalmic Res* 2021;64(1):121-127.

25 Wu H, Peng T, Zhou W, *et al*. Choroidal vasculature act as predictive biomarkers of long-term ocular elongation in myopic children treated with orthokeratology: a prospective cohort study. *Eye Vis* (*Lond*) 2023;10(1):27.

26 Liu Y, Wang L, Xu Y, *et al*. The influence of the choroid on the onset and development of myopia: from perspectives of choroidal thickness and blood flow. *Acta Ophthalmol* 2021;99(7):730-738.

27 Alonso-Caneiro D, Read SA, Collins MJ. Automatic segmentation of choroidal thickness in optical coherence tomography. *Biomed Opt Express* 2013;4(12):2795-2812.

28 Read SA, Alonso-Caneiro D, Vincent SJ, *et al*. Longitudinal changes in choroidal thickness and eye growth in childhood. *Invest Ophthalmol Vis Sci* 2015;56(5):3103-3112.

29 Alanazi M, Caroline P, Alshamrani A, *et al*. Regional distribution of choroidal thickness and diurnal variation in choroidal thickness and axial length in young adults. *Clin Ophthalmol* 2021;15:4573-4584.

30 Girard MJ, Strouthidis NG, Ethier CR, *et al*. Shadow removal and contrast enhancement in optical coherence tomography images of the human optic nerve head. *Invest Ophthalmol Vis Sci* 2011;52(10):7738-7748.

31 Insa-Sánchez G, Fuentes-Broto L, Cobos A, *et al*. Choroidal thickness and volume modifications induced by aerobic exercise in healthy young adults. *Ophthalmic Res* 2021;64(4):604-612.

32 Liang X, Wei S, Zhao S, *et al*. Investigation of choroidal blood flow and thickness changes induced by near work in young adults. *Curr Eye Res* 2023;48(10):939-948.

33 Chakraborty R, Baranton K, Spiegel D, *et al*. Effects of mild- and moderate-intensity illumination on short-term axial length and choroidal thickness changes in young adults. *Ophthalmic Physiol Opt* 2022;42(4):762-772.

34 Salchow DJ, Hwang AM, Li FY, *et al*. Effect of contact lens power on optical coherence tomography of the retinal nerve fiber layer. *Invest Ophthalmol Vis Sci* 2011;52(3):1650-1654.

35 Lee SB, Shin IH, Shin KS, *et al*. Effects of refractive power on macular thickness measurement using spectral-domain optical coherence tomography. *Ophthalmologica* 2015;234(3):172-176.

36 Yazdani N, Ehsaei A, Hoseini-Yazdi H, *et al*. Wide-field choroidal thickness and vascularity index in myopes and emmetropes. *Ophthalmic Physiol Opt* 2021;41(6):1308-1319.

37 Alanazi MK. Within-day changes in luminal, stromal choroidal thickness, and choroidal vascularity index in healthy adults. *Indian J Ophthalmol* 2023;71(1):166-173.

38 Read SA, Collins MJ, Vincent SJ, *et al*. Choroidal thickness in myopic and nonmyopic children assessed with enhanced depth imaging optical coherence tomography. *Invest Ophthalmol Vis Sci* 2013;54(12):7578-7586.

39 Walline JJ, Walker MK, Mutti DO, *et al*. Effect of high add power, medium add power, or single-vision contact lenses on myopia progression in children: the BLINK randomized clinical trial. *JAMA* 2020;324(6):571-580.

40 Zhang S, Zhang G, Zhou X, *et al*. Changes in choroidal thickness and choroidal blood perfusion in guinea pig myopia. *Invest Ophthalmol Vis Sci* 2019;60(8):3074-3083.

41 Mori K, Gehlbach PL, Yoneya S, *et al*. Asymmetry of choroidal venous vascular patterns in the human eye. *Ophthalmology* 2004;111(3):507-512.

42 Tanabe H, Ito Y, Iguchi Y, *et al*. Correlation between cross-sectional shape of choroidal veins and choroidal thickness. *Jpn J Ophthalmol* 2011;55(6):614-619.

43 Hoseini-Yazdi H, Vincent SJ, Collins MJ, *et al*. Regional alterations in human choroidal thickness in response to short-term monocular hemifield myopic defocus. *Ophthalmic Physiol Opt* 2019;39(3):172-182.

44 Moderiano D, Do M, Hobbs S, *et al*. Influence of the time of day on axial length and choroidal thickness changes to hyperopic and myopic defocus in human eyes. *Exp Eye Res* 2019;182:125-136.

45 Carracedo G, Martin-Gil A, Peixoto-de-Matos SC, *et al*. Symptoms and signs in rigid gas permeable lens wearers during adaptation period. *Eye Contact Lens* 2016;42(2):108-114.